Desalination and Water Treatment
www.deswater.com

doi: 10.5004/dwt.2022.28961

280 (2022) 60–75
December

Enhanced adsorption performance of activated carbon prepared from peanut shell for the adsorption of dyes from aqueous solution

Md. Tamez Uddin*, Md. Rukanuzzaman, Md. Akhtarul Islam

Department of Chemical Engineering and Polymer Science, Shahjalal University of Science and Technology, Sylhet-3114, Bangladesh, email: mtuddin_cep@yahoo.com/mtuddin-cep@sust.edu (Md. Tamez Uddin) ORCID: 0000-0001-9235-1112

Received 5 March 2022; Accepted 25 September 2022

ABSTRACT

In this study, activated carbon (AC) was prepared from peanut shell by activation with potassium hydroxide. The process parameters to prepare (AC) were optimized with respect to time, temperature and impregnation ration. The prepared AC was characterized by N_2 adsorption–desorption isotherms Brunauer–Emmett–Teller (BET), Fourier-transform infrared spectroscopy and scanning electron microscopy. The maximum BET surface area achieved was found to be 716 m^2/g. The AC exhibited excellent adsorption performance to methylene blue (MB). The Langmuir isotherm model was fitted well to describe the equilibrium adsorption data and the maximum adsorption capacity was achieved to be 1,388 mg/g. The adsorption followed the pseudo-second-order kinetic model. The thermodynamic study showed that the MB adsorption onto AC was exothermic and spontaneous. Considering high adsorption capacity, AC derived from peanut shells can be used as a promising adsorbent for efficient treatment of textile wastewaters.

Keywords: Activated carbon; Peanut shell; Methylene blue; Adsorption; Kinetics; Langmuir isotherm

1. Introduction

Textile-dyeing industries consume huge number of dyes, and a large portion of these dyes is disposed to the environment in form of wastewater. These dyes have high environmental impact; because they are chemically stable, non-biodegradable and potentially carcinogenic [1]. In addition, the highly colored dye-containing effluents discarded in to natural water bodies reduce photosynthesis of aquatic plants by preventing the penetration of sunlight into the water affecting the balance of aquatic ecosystems [2]. Methylene blue (MB) which is selected as a model dye in the current investigation has wider applications, which include colouring paper, temporary hair colorant, dyeing cottons, wools, and coating for paper stock. Despite the fact that methylene blue is not extremely toxic, it can have negative consequences. People who are exposed to methylene blue for a short period of time may have symptoms such as accelerated heart rate, vomiting and shock, Heinz body formation, cyanosis, jaundice, quadriplegia and tissue necrosis [3,4]. In the last decades, the dyeing industries have been flourishing in the developing countries, where economical benefit and employment-issues have priority before strict implementation of environmental laws [5–7]. Therefore, a cost-efficient wastewater treatment system needs to be developed and tailored for industrial application to prevent environmental pollution arising from synthetic dyes.

Many researchers have taken spontaneous task to develop cost-effective technology to treat the dye-containing wastewater [8–13]. The conventional methods like coagulation, flocculation, precipitation, chemical oxidation, anaerobic degradation, filtration, nanofiltration, membrane bioreactor and so on, are widely employed for the treatment of dye containing wastewater [14–16]. These existing technologies are often inefficient to reduce pollutant concentrations to anticipated level in a cost-effective and

* Corresponding author.

efficient manner. Each one has its own set of advantages and disadvantages. Chemical treatment will eliminate the coloration by destroying the chromophoric group of the dyes, but this does not always result in full mineralization [17]. Adsorption and chemical coagulation do not cause dye degradation, but they do create a waste disposal problem [18,19]. Biological treatment method, although in most cases appears to be effective owing to the favorable microorganism-growing climate, is not appealing due to the necessity of large area required for the facilities in a densely-populated country like Bangladesh and the production of large volume of sludge [20]. But even when one approach seems good, its capital costs or operating costs often make it impossible to use it in industries that need a lot of water [21]. It has become very hard to treat wastewater in a way that is both cheap and good for the environment.

Over the years, adsorption has been shown to be one of the most reliable and proven wastewater treatment methods in the textile industry because it is a cost-effective method for removing colors and decolorizing textile effluents. The adsorption process refers to the transfer of wastewater-soluble organic dyes to the adsorbent's surface, which is a solid and extremely porous substance. It is imperative that the adsorbent should be changed with fresh materials as soon as it becomes saturated with the adsorbates. Additionally, an adsorbent must have the ability to be regenerated or burnt so that it may be reused. This approach is able to extract both small and bulky organic and inorganic compounds, as well as hazardous and non-toxic substances from their solutions without producing any by-products or disintegrating the compound. Furthermore, a subsequent desorption step is able to retrieve the expensive solute molecule without compromising its composition or disrupting its structure. It has been proven that the adsorption method is superior for the treatment of water pollution since it requires less investments in terms of both the original cost and the acreage that it occupies. The equipment used for the adsorption process is simple to design and easy to operate. Therefore, adsorption might be considered a viable approach for treating wastewater, particularly if the adsorbent is economical and easily available. In the last two decades, researchers have given great attention to remove different organic pollutants from wastewaters with different adsorbents [8,14,21–26]. An efficient adsorbent must have a large specific surface area with a consistent nanoscale pore distribution in order to function properly. Activated carbon (AC) is commonly employed to remove contaminants from water or wastewater through the process of adsorption; however, one of the drawbacks of using AC is that it requires a very large initial investment. As a consequence, there is still a significant demand for research into the development of inexpensive novel AC with high adsorption capacity.

In recent decades, a large amount of research effort has been invested into the quest for ecologically benign and widely available low-cost materials that may serve as precursors in the fabrication of AC [23,25–27], leading to cheap production cost. These ACs are expected to exhibit adsorption capacity much higher than their precursor, and could undergo regeneration process at high temperature. Recently, agricultural wastes have attracted attention of many researchers to prepared AC in order to treat dye-containing wastewater [28–33]. The mesoporous AC with comparatively high surface area and pore volume was prepared from coconut husk while potassium hydroxide (KOH) was utilized as activating agent for activation [34]. The adsorption capacity of the prepared AC was investigated by the adsorption of methylene blue. The prepared AC exhibited excellent adsorption performance for the adsorption of MB with a monolayer adsorption capacity of 434.78 mg/g at 30°C. It is reported that $ZnCl_2$ activation prepared mesoporous AC that is utilized favorably for the removal of large molecules compared to AC prepared by H_3PO_4 impregnation. Pereira et al. [35] prepared cocoa shells and siriguela seeds derived AC by H_3PO_4 and $ZnCl_2$ activation in nitrogen as well as CO_2 atmosphere. The AC prepared by H_3PO_4 activation was favorable for the removal of the protein α-lactalbumin. In another study, $ZnCl_2$ impregnated AC prepared form *Hura crepitans Linn* seed shells showed higher adsorption efficiency of MB than the AC prepared by H_3PO_4 activation [36]. Furthermore, [37] walnut shells derived ACs prepared by activation showed the adsorption capacity of 315 mg/g for the MB adsorption. In addition, Nsami and Mbadcam [38] produced AC with specific surface area of 648 m^2/g from cola nut shells by $ZnCl_2$ activation which showed MB adsorption capacity of 87 mg/g. However, the trend in the present work is to produce high-capacity AC using the raw materials abundant in the locality.

Peanut shells are one of the valuable agricultural waste resources which can be used as precursor to prepare AC. Bangladesh is an agricultural country. A huge quantity of peanuts is produced in Bangladesh each year. As a by-product of peanut production, peanut shell is normally used as fuel in rural area without any commercial value and technology-added applications. Therefore, it is essential to utilize these by-products to produce a useful and a value-added product like AC. To this day, very little information has been published regarding an effective and straightforward method of producing AC from peanut shell and employing it as a possible adsorbent for the treatment of textile effluents that contain organic colors [39–41]. In addition, the effect of process parameters on AC production yield has not been well investigated.

The purpose of the present work was to prepare AC from peanut shell by KOH activation and explore the feasibility of using this AC as adsorbents to treat dye containing wastewaters. The influences of different activation parameters on the percentage yield of AC as well as its adsorption performance have been studied. The as-prepared AC was characterized by various techniques. The different adsorption parameters for the removal of a cationic dye MB were studied in order to evaluate the adsorption capacity of the as-prepared AC.

2. Material and methods

2.1. Materials

Peanut shells, disposable part of commercial product 'peanuts', were collected from a local market in Sylhet, Bangladesh, and used as raw materials for the production of AC. All working solutions of methylene blue (MB) were

prepared by diluting the stock solution of concentration 1,000 mg/L with adding distilled water to the prescribed concentration. The solutions of desired pH were obtained by adding 0.1 M HCl or 0.1 M NaOH solutions. All chemicals utilized in this work were of analytical grade and used as received without further purification.

2.2. Preparation of AC

The peanut shells collected from the local market were washed with distilled water to remove dust and dirt, dried at 110°C and then crushed to desired particle size. The crushed peanut shells were then impregnated with activating agent KOH at different activating agent/precursor ratio by mass under vigorous stirring for 24 h at room temperature. It was then filtered and dried in an oven at 120°C for 24 h. Subsequently, the impregnated precursor (of known weight) is transferred to a stainless-steel reactor (18 cm length and 4.5 cm diameter) with narrow ports at both ends prepared locally. An inert medium inside the reactor was created by purging N_2 through the reactor. After purging both ends of reactor was closed and the reactor was placed inside a muffle furnace for carbonization at different temperature and holding time. The activated samples were then washed several times with distilled water until the pH of the washing solution reached 7. Finally, the samples were dried in an oven at 105°C for 24 h and stored in glass containers. Impregnation ratios varying from 0.5 to 1.5 and holding time of 1 h to 3 h and carbonization temperature of 400°C–700°C were tried and the yield of the resultant carbon was determined.

Peanut shells, disposable part of commercial product 'peanuts', were collected from a local market in Sylhet, Bangladesh, and used as raw materials for the production of AC. The cost of the collected raw peanut shells was thus omitted from the analysis of the total costs. The cost of consumables was calculated by budgeting quotes for these consumables that were acquired from several vendors. Industrial energy price from the local electricity source (Bangladesh Power Development Board (BPDB), Sylhet) was used to evaluate necessary utility services. The drying oven and the electric furnace are the two pieces of equipment that use the most electricity. The cost of producing activated carbon from peanut shell in the laboratory was determined to be USD 2.95/kg which was comparable to the estimated cost of producing iron based metal organic framework described elsewhere [42].

2.3. Characterization of the precursor and the AC

The following physical and chemical parameters of the precursor and the AC have been determined:

- Chemical composition: This parameter was represented by lignin-, hemi-cellulose-, cellulose-, and extractive components-content of the peanut shells and was determined by conventional analytical methods [43].
- Specific surface area and pore-size distribution: These parameters of the peanut shell powder and the prepared AC were determined by N_2 adsorption–desorption isotherms at 77 K (ASAP-2020 Plus, Micromeritics Instrument Corporation, USA). Before each analysis, the samples were degassed at 120°C in vacuum for a time interval long enough to reach a constant pressure less than 10 μm Hg. The specific surface areas (S_{BET}) were calculated using the Brunauer–Emmett–Teller (BET) equation between 0.06 and 0.3 relative pressure (P/P_0). Mesopore size distributions were obtained from the Barrett–Joyner–Halenda (BJH) method [44] applied to the adsorption course of the nitrogen adsorption isotherm. The calculation was performed by the Micromeritics software package which used the recurrent method and applied the Harkins–Jura equation for the multilayer thickness estimation [45].
- Surface texture of AC: The surface and the pore-structure of the peanut shell powder and the prepared AC were studied by scanning electron microscope (SEM).
- Functional groups: The functional groups on the AC surface were determined from a Fourier-transform infrared spectroscopy (FTIR) spectra (acquired by FTIR spectroscope, Shimadzu IR, Japan). The samples were diluted with KBr and pressed to form a disk-shaped compact mass prior to FTIR analysis. FTIR spectra were measured in the frequency ranging from 450 to 4,000 cm^{-1}.
- pH at point of zero charge, pHpzc: This parameter of the prepared AC was determined by pH drift method. Typically, solutions of different initial pH (2–10) were prepared in 50 mL plastic Erlenmeyer flasks. To the solutions with adjusted pH, 0.2 g of AC was added and the suspensions were shaken with a flash shaker and allowed to equilibrate for 24 h at room temperature. After 24 h, the suspensions were separated by filtration and the final pH values of the supernatant liquid were measured. The pH_{pzc} was determined from point of intersection of the plot initial pH_i vs. change in pH values (ΔpH) at which ΔpH is 0.
- Determination of methylene blue number: The methylene blue number is defined as the maximum amount of dye adsorbed on 1.0 g of adsorbent. Therefore, it is the concentration of dye in the solid phase. It is also described in the literature as q_e. In order to determine the methylene blue number of the prepared AC 0.10 g of AC were stirred with 200.0 mL methylene blue solution of initial concentration 600 mg/L for 4 h. The solution was then centrifuged and remaining concentration of methylene blue was analyzed using a UV/Vis spectrophotometer (Model UV-1601, Shimadzu Corporation, Japan). The methylene blue number was determined by the Eq. (1):

$$\mathrm{MB}_N = \frac{\left(C_0 - C_e\right)V}{W} \tag{1}$$

where C_0 (mg/L) is initial concentration, C_e (mg/L) is equilibrium concentration, V (L) is volume of solution and W (g) is the amount of AC.

2.4. Batch adsorption study

2.4.1. Effect of pH

The effect of pH on the adsorption intensity of methylene blue was studied over the pH range of 2–10. A series

of 100 mg/L methylene blue solutions at various initial pH (2–10) were prepared by the addition of either HCl or NaOH. 200 mL of each of these methylene blue solutions was taken in Erlenmeyer flask containing 0.1 g AC and was shaken for 4 h using flash shaker at a constant oscillation of 400 osc/min. The adsorbent was then separated from the aqueous phase by centrifugation. The concentrations of MB were determined using a double beam UV-Visible spectrophotometer (UV-1601 Shimadzu, Japan) at 664 nm.

2.4.2. Effect of adsorbent dosages

The effect of AC dosages on the adsorption capacity of AC MB was investigated by adding 0.1–0.5 g ACs into a series of 250 mL Erlenmeyer flask each filled with 200 mL of MB solution of 200 mg/L. Each sample was then shaken for 4 h at a constant oscillation of 400 osc/min. The samples were then centrifuged and the concentrations of MB remaining in the supernatant were then analyzed as before.

2.4.3. Adsorption isotherm study

Equilibrium studies were performed by adding 0.1 g of AC to 200 mL of MB solution of concentrations 200, 300, 400, 500 and 600 mg/L in 250 mL Erlenmeyer flasks. Adsorption equilibrium was attained by shaking the flask for 4 h was sufficiently high for the attainment of adsorption equilibrium followed analysis the samples as before. The adsorption capacity (defined as concentration of MB in the solid phase, mass/mass) at equilibrium, q_e (mg/g), was calculated by:

$$q_e = \frac{(C_0 - C_e)V}{W} \tag{2}$$

where C_0 and C_e (mg/L) are the liquid-phase concentrations of the dye at initial and equilibrium conditions, respectively, W is the amount of adsorbent in g and V is the volume of the solution in mL. Similar equilibrium study was performed at different temperatures in order to investigate the effect of temperature on the adsorption of methylene blue onto the prepared AC.

2.4.4. Kinetic study

Kinetic study was performed following the similar procedure as isotherm study changing the concentration in the range of 200–500 mg/L while keeping the solution volume and adsorbent dosage constant. MB solutions at preset time intervals was collected by disposable syringes and the concentrations were then determined as before. The adsorption capacity at time t, q_t (mg/g) was calculated by the following equation:

$$q_t = \frac{(C_0 - C_t)V}{W} \tag{3}$$

where C_0 and C_t (mg/L) are the liquid-phase concentrations of dye at initial and at any time t, respectively.

3. Results and discussion

3.1. Characterization of the peanut shell

The proximate analysis and the determination of lignocellulosic component in the peanut shell precursor were studied in order to know its quality for the production of AC as the porous structure of the prepared AC is determined by the lignocellulosic components content in precursor. The precursors with high contain of cellulose and lignin percentages contribute high yield and porous nature of the produced AC [46]. The proximate analysis of peanut shell confirmed the fixed carbon content of 21.95 wt.%, volatile content 71.15 wt.% and ash content 4.80 wt.%. Component analysis revealed that the cellulose content in the peanut shells with dry basis component mass was as high as 41.02 wt.% and the lignin-content was the second richest group with 32.87 wt.%. It was reported that agricultural solid like peanut shells possessing high percentage of cellulose and lignin could be utilized to prepare AC of enhanced surface area [47,48].

3.2. Optimization of activation parameters

The important variable that should be considered to produce AC from its precursor is its yield. It is defined as the amount of AC formed per unit mass of peanut shell and is expressed in percentage. It is essential to have high yield for feasible cost-effective production of AC. The important variables to have high yield of AC include activation time, temperature and impregnation ratio. Results for percentage yield of AC prepared at various activation conditions are shown in Table 2. The yield of AC increased from 40.10% to 78.34% when the impregnation ratio was increased from 0.5:1 to 1.5:1. Inhibition of tar formation and fast pyrolytic decomposition are considered as reasons for higher yield of carbon with increasing impregnation ratio [49]. The chemical activating agent, KOH, also may act as a barrier to protect the internal carbon structure and prevents the production of volatile products from excessive burn-off [50].

The yield of AC was also affected by activation temperature. Table 1 shows that the yield of the AC decreased monotonously from 71.39% to 56.29% with increasing temperature from 400°C to 700°C. This low yield of AC was due to the release of more volatile components as a result of enhanced rate of reaction between carbon and KOH at a higher temperature with simultaneous development of pores in AC [51,52]. Similar trend was reported by previous authors [53,54].

The development of porous structure and the yield of AC were also affected by activation time. Table 1 demonstrates that the AC yield decreased from 83.29% to 64.30% when the activation time was increased from 1 to 4 h. This was due to higher carbon burn-off at longer retention time [55]. In the present study, the activation process parameters were optimized by MB number which is an indication of the performance of AC as adsorbent.

The effects of various carbonization parameters on the MB number are shown in Fig. S1A–C and Table 1. As seen in Table 1, the methylene blue number increased from 353 to 511 mg/g with increasing the impregnation ratio from 0.5:1

to 1:1 keeping other parameters such as carbonization temperature and time constant at 500°C and 4 h, respectively; but decreased after further increase in impregnation ratio from 1:1 to 2:1. In this range, the methylene blue number reduced from 511 to 396 mg/g. Thus, the maximum MB number was achieved at impregnation of 1:1. In the course of activation, potassium hydroxide was responsible for the degradation of organic materials releasing volatile matter and simultaneously developing void and porous structure resulting higher MB number. In addition, KOH reacts with C under nitrogen atmosphere leading to the formation of K_2O, K and K_2CO_3 in the course of the activation. Diffusion of these compounds through the structure of hydrochar create new pores and make the existing pore larger [56]. Similar effects were reported by other authors as well [57,58].

At the optimum impregnation ratio of 1:1, the carbonization was accomplished at various temperatures (400°C–700°C) for 3 h. The obtained AC demonstrated highest MB number of 572 mg/g at 500°C (Table 2). This highest value of MB number clearly indicated that 500°C was the optimum temperature for the activation of peanut shell for AC formation.

The impregnated peanut shell was carbonized for different time interval (1–4 h) at optimum impregnation ration and activation temperature. The MB number increased up to activation time 3 h which decreased further on the increase in activation time. Thus, the highest MB number was found to be 572 mg/g for the AC carbonized for 3 h. The MB number reduced owing to the formation of mesopores resulting from widening of micropores [59]. From these results, it is concluded that the carbonization of peanut shell with impregnation ratio of 1:1 at 500°C for 3 h were the optimum conditions for the production of AC.

3.3. Characterization of AC

3.3.1. Surface area and pore-size distribution

Information about the adsorption mechanism and the porous structure of AC are primarily obtained from the shape of adsorption isotherm [60]. The N_2 adsorption/desorption isotherms of ACs prepared from peanut shell is given in Fig. S2A to explain general features of AC. The nitrogen adsorption isotherm clearly showed that the prepared AC was a composite of micro-mesoporous in nature. The micro-mesoporous nature of the prepared AC was further confirmed by pore-size distribution (Fig. S2B).

The textural properties of the prepared AC are represented in Table 2. The BET specific area was observed to be 716 m^2/g and surface area of pores were estimated as 253 and 287 m^2/g, respectively. The surface area of the peanut shell powder before activation was found to be 0.83 m^2/g. The total pore volume was 0.63 cm^3/g at relative pressure (P/P_0) of 0.985 while the average pore diameter was found to be 6.5 nm. The average adsorption pore diameter of peanut shell powder before treatment with KOH was 7.98 nm. The adsorbate can easily be adsorbed if the diameter of the adsorbate is 1.7 times smaller than that of adsorbent pore diameter. As the diameter of MB is about 0.8 nm, the prepared AC could easily adsorb MB molecules [61].

3.3.2. Scanning electron micrograph analysis of AC

Scanning electron microscopy (SEM) was employed to investigate the surface morphology of the prepared AC and peanut shell powder before activation with KOH. Very few big pores were present in the peanut shell powder before it was treated with KOH, as indicated by the SEM image presented in Fig. S3. SEM micrographs as displayed in Fig. 1 clearly demonstrate that after activation pores with

Table 2
Textural properties of peanut shells derived AC

BET surface area (S_{BET})	716 m^2/g
Langmuir surface area (S_{Lang})	1,077 m^2/g
Micropore surface area (S_{mic})	402 m^2/g
External surface area (S_{ex})	314 m^2/g
Total pore volume (V_T)	0.276 cm^3/g
Micropore volume (V_{mic})	0.213 cm^3/g
Mesopore volume (V_{mes})	0.063 cm^3/g
V_{mic}/V_T	77.17%
Average pore diameter (D_p)	6.5 nm

Table 1
Optimization of activation parameters for the preparation of AC from peanut shell with KOH activation

Sample No.	Carbonizing temperature (°C)	Activation time (h)	Impregnation ratio	Yield (%)	Methylene blue number (mg/g)
KOH# 01	500	4	0.5:1	40.10	353
KOH# 02	500	4	1:1	64.30	511
KOH# 03	500	4	1.5:1	78.34	447
KOH# 04	500	4	2:1	68.65	396
KOH# 05	500	1	1:1	83.29	393
KOH# 06	500	2	1:1	74.29	491
KOH# 07	500	3	1:1	67.46	572
KOH# 08	400	3	1:1	71.39	451
KOH# 09	600	3	1:1	63.43	532
KOH# 10	700	3	1:1	56.29	511

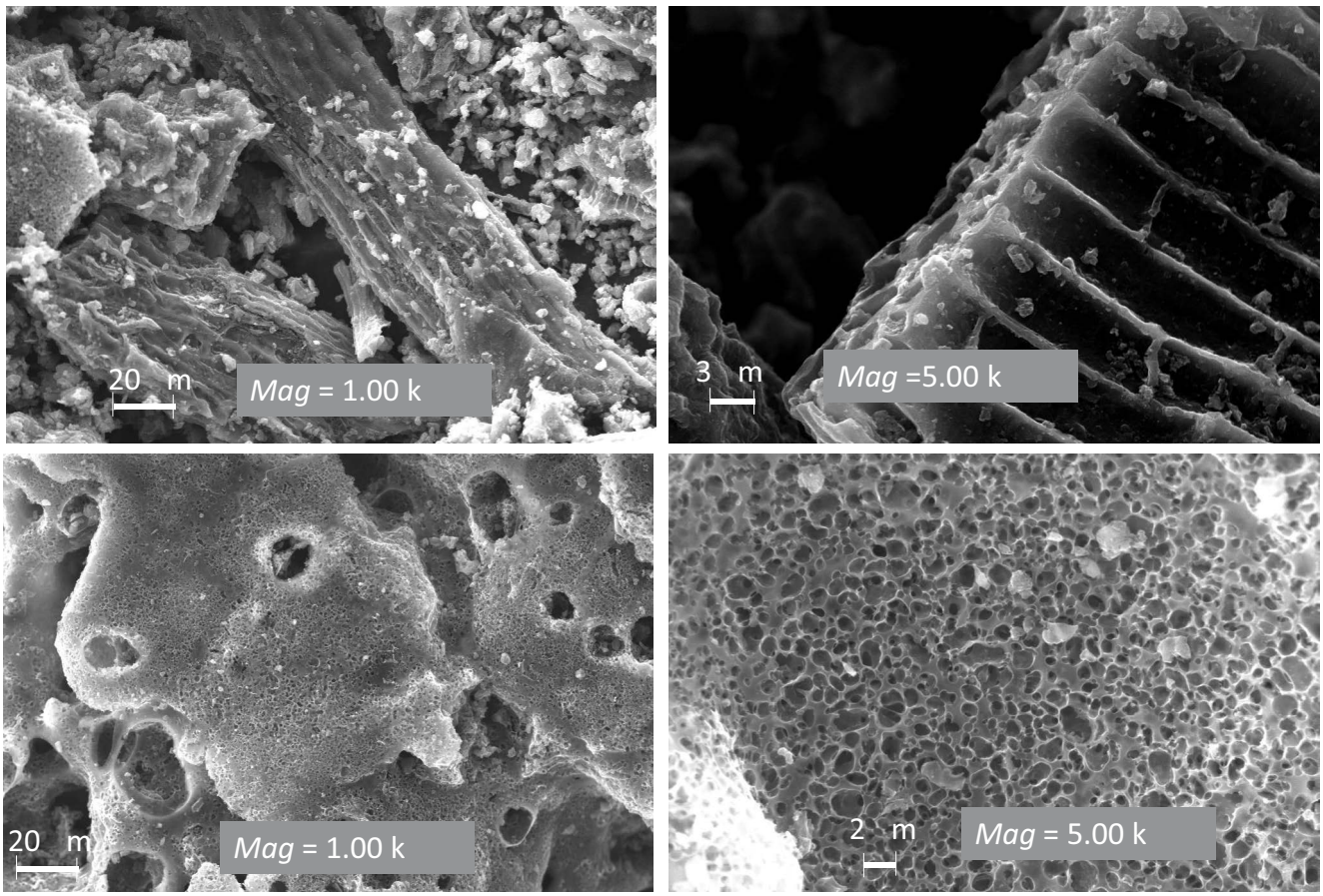

Fig. 1 Scanning electron micrograph of AC from peanut shell prepared under optimum conditions (activation temperature =773 K, activation time = 3 h and impregnation ratio = 1:1)

different sizes were developed. The asymmetrical pores in the outer surface of AC confirmed the presence of internal meso-micropores of AC. Formation of the pores was due to the intercalation of *K* formed during activation [62].

3.3.3. FTIR analysis

The functional groups of the as-prepared AC were investigated using FTIR technique. The FTIR spectra of peanut shell derived AC prepared at optimum process parameters is shown in supplementary information (Fig. S4). Four noticeable peaks were observed in the FTIR spectra of AC. A broad band ranging from 3,200 to 3,500 cm^{-1} was ascribed to the O–H stretching vibration of hydroxyl groups. The peak at 2,355 cm^{-1} corresponded to the N–H or the C=O stretching vibrations. An absorption at 1,570 cm^{-1} indicated the presence of aromatic ring or C=C stretching vibration [63]. The C=O and C–O of carboxylic groups [64] or in-plane vibration of O–H of carboxylic group [65] were confirmed by the absorption peak at frequency 1,400 cm^{-1}.

3.3.4. Determination of pH_{pzc} of the AC

At the point of zero charge ($pH_{pzc)}$, the amount of acidic and basic functional groups on the adsorbent surface is equal. Fig. 3 shows the plot of the difference of pH ($\Delta pH = pH_i - pH_f$) vs. initial solution pH. From Fig. 2A it was apparent that the graph intersected the abscissa at pH 6.4 ± 0.2, and thus at pH 6.4 ± 0.2 the surface charge of the prepared AC became neutral. Hence the pH_{pzc} of the AC adsorbent was estimated to be 6.4 ± 0.2.

3.4. Adsorption study

3.4.1. Effect of pH on adsorption

The removal of dye by adsorption is strongly affected by the nature of adsorbent active sites and the chemistry of adsorbate in aqueous media which in turn is largely depended on solution pH. The adsorbent surface charge and the extent of ionization of adsorbate molecules is affected by solution pH [66]. As the H^+ and OH^- ions are relatively strongly adsorbed, the change in solution pH, therefore, affects the adsorption of other ions.

The effect of pH on the adsorption performance of AC for MB adsorption is shown in Fig. 2B. The removal of MB increased from 22% to 97% and the equilibrium adsorption capacity increased from 43 to 193 mg/g with increasing initial solution pH from 2.0 to 10.0. The MB adsorption on AC was nearly constant at pH higher than 9.0. Removal of dye suddenly increased after pH range 6.4. This could be explained by the electrostatic interaction of between

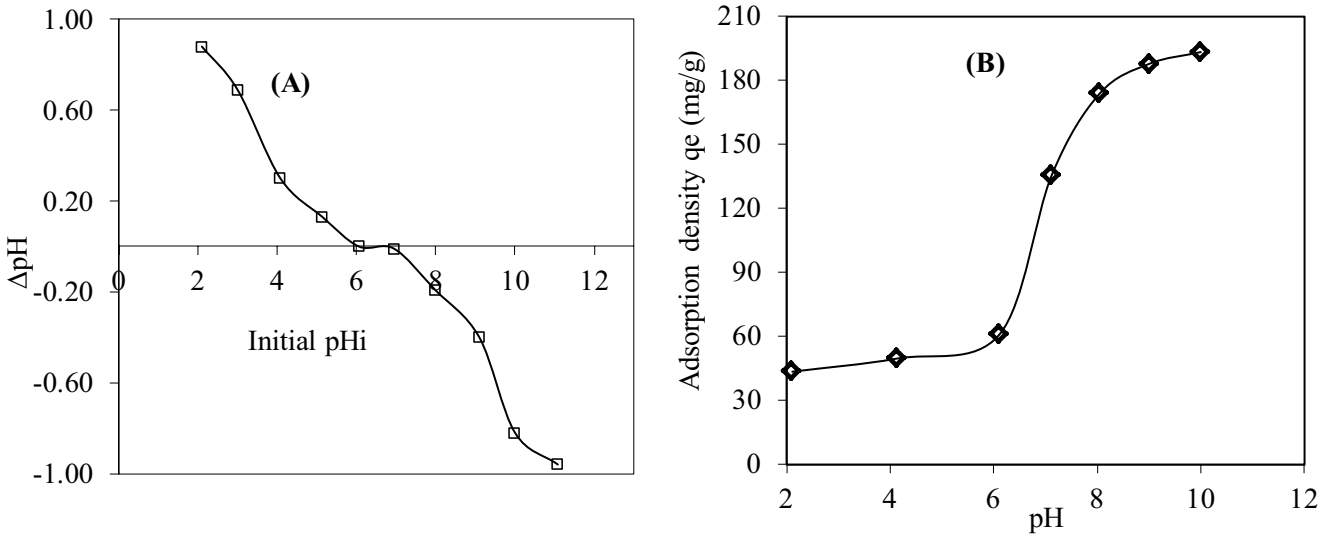

Fig. 2. (A) pH_{pzc} of AC produced from peanut shell and (B) effect of pH on the removal of methylene blue onto AC (C_0 = 100 mg/L; V = 200 mL; W = 0.1 g; T = 301 ± 2 K).

positively charged dye and negatively charged active sites on AC. The number of negatively charged sites on AC increased with increasing pH which enhanced the attraction force between dyes and negatively charged active sites on AC resulting higher adsorption capacity. The excess H^+ ions were strongly adsorbed on AC at lower pH compared to the dye molecules leading to the lower adsorption capacity of AC. In addition, the surface of AC got positive charge at low pH due to the adsorption of H^+ ions which prevented the adsorption of MB by electrostatic repulsion force. The enhanced adsorption capacity higher pH could also be explained with respect to pH_{pzc}. The pH_{pzc} of AC was found to be 6.4 ± 0.2 (Fig. 2A). At pH < pH_{pzc}, AC surface became positively charged due to the adsorption of H^+. This created a strong force of repulsion between the cationic dye MB and the positive charged AC surface which resulted in low adsorption. The reverse situation happened when the pH of the solution was higher than pH_{pzc}. At pH > pH_{pzc}, the surface of the AC became negative negatively charged by the adsorption of OH^- leading to increased removal of methylene blue (cationic dye) through electrostatic forces of attraction. Similar results were observed for the adsorption of methylene on mango leaf powder [67], jackfruit leaf powder [68], tea waste [3], coconut coir dust [69], and on pine core biomass [70].

3.4.2. Effect of contact time and initial concentration

The effect of contact time on adsorption capacity of AC for MB was investigated at its different initial concentrations. The results are presented in Fig. 3A. It is evident from Fig. 3A that the MB adsorption capacity was increased with increase in contact time at all initial concentrations. Fig. 3A demonstrates that the adsorption was very fast in the initial stage (up to 70 min) and the equilibrium adsorption was attained in about 200 min. About 75% ± 5% of the total adsorption was took place in the first rapid phase (70 min) and the subsequent adsorption rate was found to be decreased. The enhanced adsorption rate at the initial period was due to increased concentration gradient between adsorbate in solution and that on the adsorbent surface because most of the active sites on the adsorbent remain vacant at the initial stage [67]. As the time proceeded, the MB occupied the vacant sites resulting reduction of concentration gradient and thus the adsorption rate was decreases in succeeding stages from 70 to 300 min. These kinetic experiments confirmed that the adsorption of MB dye on the prepared AC was more or less two-step process: firstly, a very rapid adsorption of dye from the bulk to the external surface of the adsorbent; secondly, slow intraparticle diffusion in the interior of the adsorbent pores. Fig. 3A also displays that the adsorption capacity of AC for MB increased with initial concentration of MB. The adsorption capacity for MB increased from 246 to 504 mg/g as the MB concentrations increased from 200 to 500 mg/L which resulted from increased concentration gradient at higher initial dye concentration [71]. The increase in initial concentration also enhanced the interaction between adsorbent and dye [72]. On the other hand, at lower concentration, the active sites on the adsorbent surface remained unoccupied resulting lower adsorption capacity.

3.4.3. Effect of dosages on adsorption capacity

The effect of AC dosages on the amount of dye adsorbed was investigated by performing adsorption experiments in 200 mL MB solution of concentration 200 mg/L containing different dosages of AC keeping other parameters constant (Fig. 3B). Fig. 3B exhibits that the adsorption capacity changed with AC dosage and was decreased with the increase in AC dosages. The adsorption capacity reduced from 195 to 68 mg/g when the AC dosages was increased from 0.1 to 0.5 g. This might be explained with the availability of the dye molecules. The number of adsorption active sites on AC in a fixed amount of solution depends on the dosages of AC. Usually higher the dosage higher is the adsorption sites.

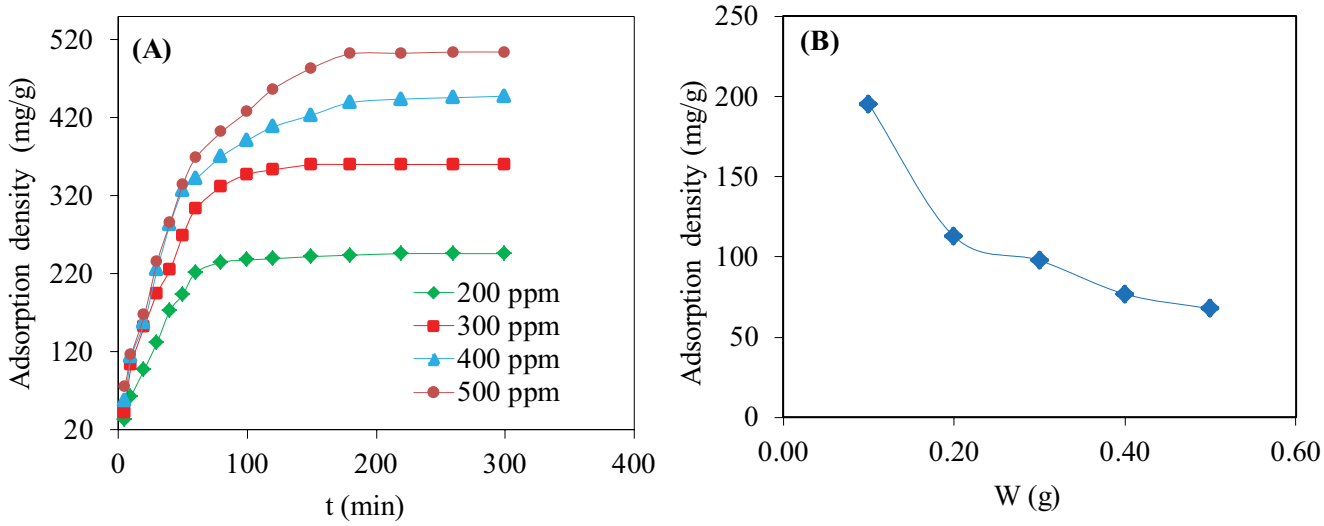

Fig. 3. (A) Effect of contact time and initial concentrations on the adsorption of methylene blue onto AC (C_0 = 200, 300, 400, and 500 mg/L; W = 0.1 g; V = 200 mL; pH = 6.8; T = 28°C ± 2°C) and (B) effect of AC mass on adsorption capacity (C_0 = 200 mg/L; pH = 6.8; V = 200 mL; T = 301 ± 2 K).

Consequently, all the adsorption active sites on AC were not occupied at high adsorbent dosages due to lack of MB dyes resulting in lower adsorption capacity. At higher dosage of AC, the surface area was also reduced due the aggregation of AC which also resulted in lower adsorption capacity [73].

3.4.4. Adsorption isotherms

Adsorption isotherms are generally utilized to report the adsorption data and describe the interaction of solutes with adsorbents. Isotherms portray the amount of a molecule adsorbed at different concentrations but at constant temperature. The maximum adsorption capacity of adsorbent for a given adsorbate is determined by equilibrium isotherm experiment [74]. Experimental data of equilibrium adsorption isotherms can be explained with several models reported in literature [75]. In the present study, Langmuir and Freundlich isotherm models have been used to describe isotherm experimental data.

The Langmuir isotherm assumes that once a adsorption site is occupied by a molecule of dye, no further molecule can be adsorbed at that site [76] indicating the maximum adsorption of dyes onto AC surface is achieved when the surface becomes saturated. The Langmuir isotherm model is expressed as [77]:

$$q_e = \frac{q_0 K_L C_e}{1 + K_L C_e} \tag{4}$$

Taking reciprocal, the above equation can be written as

$$\frac{1}{q_e} = \frac{1}{q_0} + \frac{1}{q_0 K_L} \cdot \frac{1}{C_e} \tag{5}$$

where C_e, q_e are equilibrium concentration (mg/L), adsorption capacity of adsorbent (mg/g) at equilibrium, respectively; q_0 and K_L are Langmuir constants. Intersect and the slope of the plot $1/q_e$ vs. $1/C_e$ are used to determine the Langmuir constant q_0 and K_L, respectively.

On the other hand, the Freundlich isotherm assumes heterogeneous adsorption surface [78] and is given as:

$$q_e = K_F C_e^{1/n} \tag{6}$$

Taking logarithm gives the linear form of Eq. (5) as:

$$\ln q_e = \ln K_F + \frac{1}{n} \ln C_e \tag{7}$$

where n and K_F are the Freundlich constants indicating adsorption intensity and adsorption capacity, respectively. The value of K_F and n can be estimated from the plot $\ln q_e$ vs. $\ln C_e$.

Fig. 4A and B show the Langmuir and Freundlich curves for MB adsorption onto AC, respectively. The isotherm parameters are presented in Table 3. Table 3 demonstrates that the Langmuir isotherm was fitted better of experimental data than Freundlich isotherm which was evidenced by the correlation coefficients as correlation regression coefficient of Langmuir isotherm was higher (0.99) than that of Freundlich isotherm (0.971). These results strongly suggested that there was monolayer coverage of MB dye molecule on the AC surface. The maximum adsorption capacity of AC for MB adsorption was obtained to be 1,388 mg/g which was higher than that of AC prepared from various low-cost cellulosic materials for MB adsorption stated elsewhere as listed in Table 4. It is obvious from Table 4 that the peanut shell derived AC in this study exhibited enhanced adsorption capacity (1,388 mg/g) for the adsorption of MB as compared to others cited in the literature.

3.4.5. Adsorption kinetics

The adsorption kinetic is important for designing and modeling of industrial adsorption columns. The mechanism of

Table 3
Langmuir and Freundlich constants for the adsorption of methylene blue onto prepared AC

Langmuir isotherm			Freundlich isotherm		
K_L (L/mg)	q_0 (mg/g)	R^2	K_F (mg/g)(mg/L)$^{1/n}$	n	R^2
0.213	1,388	0.990	6.755	1.468	0.974

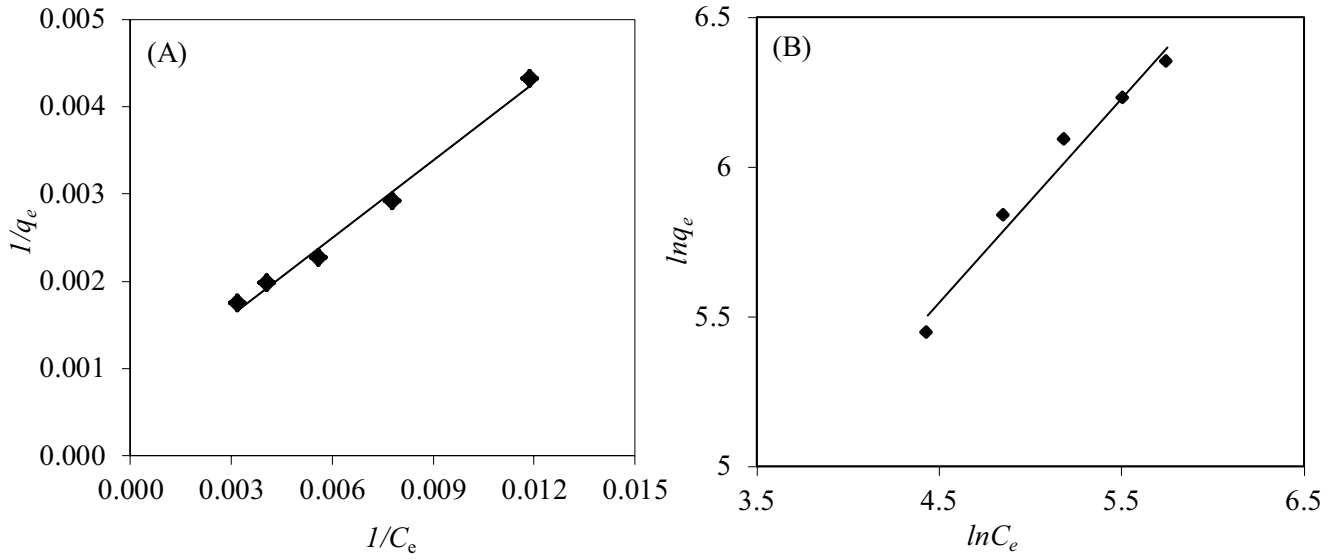

Fig. 4. (A) Langmuir isotherm and (B) Freundlich isotherm for methylene blue adsorption onto AC. (C_0 = 200–600 mg/L; pH = 6.8; V = 200 mL; W = 0.1 g; T = 301 ± 2 K).

Table 4
Adsorption capacity of AC prepared from different lignocellulosic materials for methylene blue adsorption

Adsorbents	Adsorption capacity q_0 (mg/g)	References
Rattan hydrochar-based AC	359	[79]
Elaeagnus stone-based AC	288	[80]
Tea waste-based AC	402	[81]
Hazelnut husk-based AC	476	[82]
Tea seed-based AC	325	[83]
Pecan nutshell-based AC	400	[84]
Cotton stalk-based AC	192	[85]
Periwinkle shells-based AC	500	[86]
Rattan sawdust-based AC	294	[87]
Oil palm-based AC	909	[88]
Co-doped Fe-BDC MOF	2.95	[89]
Fe-BDC MOF	8.65	[90]
Peanut shell-based AC	1,388	Present study

solute sorption onto a sorbent can be described with different models. To study the adsorption kinetic is essential for a fast and effective design of model for the adsorption column. The pseudo-first-order [91] and pseudo-second-order [92] kinetic models were used to examine the dynamics in this study due to their good applicability in most cases in comparison with the other models.

The pseudo-first-order kinetic model assumes that adsorption rate of solutes is proportional to the quantity of unoccupied sites. The differential form of the pseudo-first-order model is usually written as:

$$\frac{dq}{dt} = k_1\left(q_e - q\right) \tag{8}$$

After integration by applying conditions, $q = 0$ at $t = 0$ and $q = q$ at $t = t$, Eq. (8) can be written as:

$$\ln\left(q_e - q\right) = -k_1 t + \ln q_e \tag{9}$$

where q_e and q are the adsorption capacity (mg/g) of AC for MB adsorption at equilibrium and at time t (min), respectively, and k_1 is adsorption rate constant (min^{-1}). A plot of $\ln(q_e - q)$ vs. t is a linear with the slope k_1 and intercept $\ln q_e$.

The pseudo-second-order kinetic model predicts the behavior for the adsorption process for all dye concentrations. This model is also used to predict chemisorption processes. The second-order kinetic equation is expressed as:

$$\frac{dq}{dt} = k_2\left(q_e - q\right)^2 \tag{10}$$

After integration, Eq. (10) can be written as:

$$\frac{t}{q}=\frac{1}{k_2 q_e^2}+\frac{1}{q_e}t \tag{11}$$

where k_2 (g/mg·min) is pseudo-second-order rate constant. The plot of t/q vs. t of Eq. (11) is linear, the slope and intercept of which is used to determine q_e and k_2, respectively.

Linearized plot of Eqs. (9) and (11) are represented in Fig. 5A and B, respectively. The pseudo-first-order and second-order kinetic parameters are presented in Table 5. Table 5 shows that the pseudo-second-order kinetic model was fitted well compared to first order model as the correlation coefficients for pseudo-second-order model (0.99) was higher than that of pseudo-first-order model (<0.96) and the calculated adsorption capacity $q_{e,cal}$ were close to the experimental $q_{e,exp}$ values. Thus, the pseudo-second-order kinetic model well described the kinetic for the adsorption of MB onto AC.

3.4.6. Thermodynamic study

The feasibility of the adsorption of methylene blue onto the as-prepared AC was investigated by performing a thermodynamic study. The spontaneity of process is determined by the change in Gibbs free energy (ΔG), the negative values imply a spontaneous process [72]. The exothermic/endothermic nature of the process and the magnitude of changes in the adsorbent surface are predicted by the enthalpy change (ΔH) and entropy change (ΔS), respectively [93]. The change in ΔG is determined using the following equation:

$$\Delta G=-RT\ln K_D \tag{12}$$

The values of ΔH and ΔS are determined using the Van't Hoff equation [Eq. (13)]:

$$\ln K_D=-\frac{\Delta H}{R}\left(\frac{1}{T}\right)+\frac{\Delta S}{R} \tag{13}$$

where R is the universal gas constant, T is the temperature in Kelvin, and K_D is equilibrium constant. The values of ΔS and ΔH can be obtained from the plot $\ln K_D$ vs. $1/T$.

Plot of $\ln K_D$ vs. $1/T$ for the estimation of the thermodynamic parameters for MB adsorption using prepared AC is shown in supporting information (Fig. S5). The thermodynamic parameters ΔG, ΔH and ΔS are presented in Table 6. According to Table 6, the values of ΔG at 293 and 303 in adsorption of MB are negative in all cases

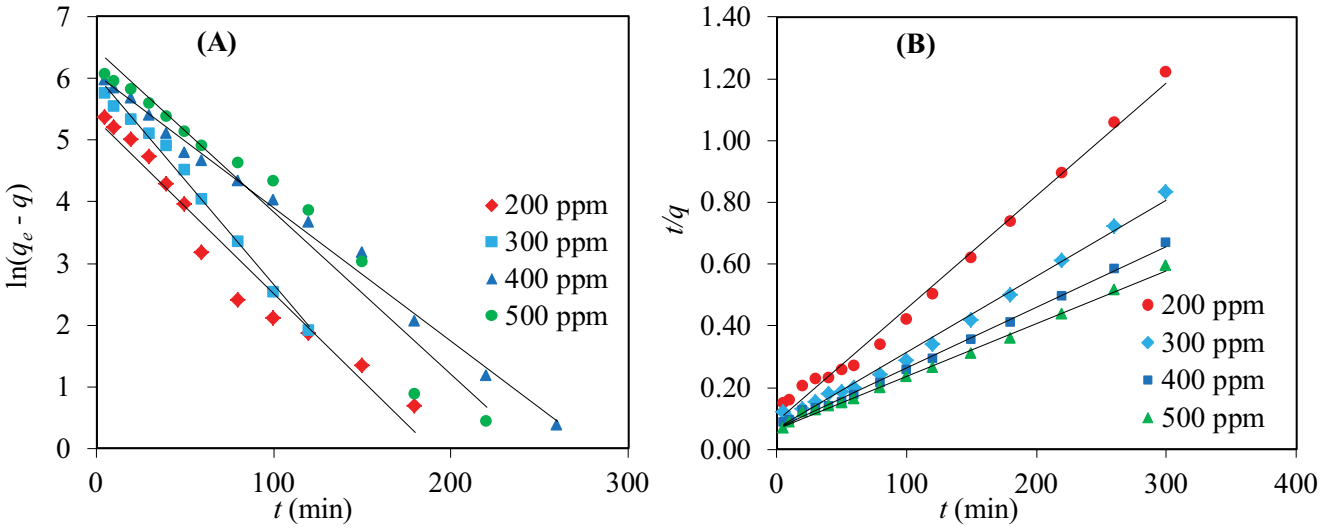

Fig. 5. (A) Pseudo-first-order kinetics and (B) pseudo-second-order kinetics for the adsorption of methylene blue on AC (C_0 = 200, 300, 400, and 500 mg/L; W = 0.1 g; V = 200 mL; pH = 6.8; T = 28°C).

Table 5
Pseudo-first-order and pseudo-second-order kinetic parameters for the adsorption of MB on AC

		Pseudo-first-order model			Pseudo-second-order model		
C_0 (mg/L)	$q_{e,exp}$ (mg/g)	k_1 (min^{-1})	$q_{e,cal}$ (mg/g)	R_1^2	k_2 (g/mg·min)	$q_{e,cal}$ (mg/g)	R_2^2
200	246	0.028	205	0.956	2.89×10^{-4}	244	0.998
300	360	0.041	560	0.950	8.9×10^{-5}	366	0.992
400	447	0.021	627	0.943	5.7×10^{-5}	450	0.997
500	504	0.026	642	0.955	4.4×10^{-5}	508	0.996

Table 6
Thermodynamic parameters for the adsorption of methylene blue on AC

C_0 (mg/L)	T (K)	ΔG (kJ/mol)	ΔH (kJ/mol)	ΔS (kJ/mol·K)	R^2
	293	–3.688			
200	303	–2.538	–56.02	–0.177	0.984
	323	1.551			
	293	–3.332			
300	303	–2.177	–54.01	–0.172	0.986
	323	1.757			
	293	2.524			
400	303	–2.188	–52.69	–0.169	0.924
	323	2.355			
	293	–1.975			
500	303	–1.759	–46.82	–0.151	0.913
	323	2.370			

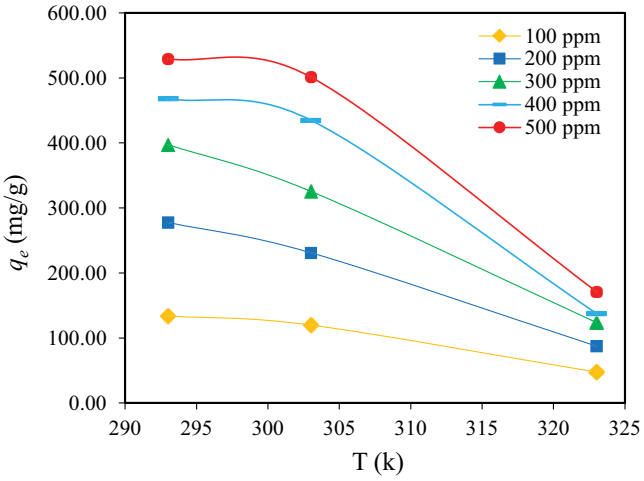

Fig. 6. Effect of temperature on adsorption capacity of methylene blue on AC (C_0 = 100–500 mg/L; pH = 6.8; V = 200 mL; W = 0.1 g).

confirming that the process was spontaneous. Whereas at 323 K, the value of ΔG is positive which confirmed that adsorption was favorable at low temperature. The negative value of ΔH ranging from –56.02 to –46.82 kJ/mol (Table 6) indicated exothermic nature of adsorption whereby no energy input from outside of the system is required. As the process was exothermic, one *would* expect the reduction of adsorption capacity with increasing temperature. This was *confirmed* by investigating the adsorption of MB onto AC at various temperatures (Fig. 6). From Fig. 6, it was obvious that the adsorption capacity decreased with increasing temperature which agreed well with the conclusion obtained from the values of ΔH. The decrease in the randomness at the solid/liquid interface in course of MB adsorption onto AC was evidenced by the negative ΔS value [94].

4. Conclusion

A batch adsorption experiment was carried out in order to investigate the potentiality of peanut shell derived for the adsorption of MB under different experimental conditions. The as-prepared AC was found to be effective for adsorption of MB as proved by experimental results. The AC prepared was micro-mesoporous with specific surface area of 716 m^2/g. The adsorption capacities of AC for MB were changed with contact time, solution pH and dye concentrations. The adsorption capacity of AC for MB was higher at basic media in comparison to acid media. The adsorption capacity (mg/g) was increased with contact time and increasing initial solution concentration. Equilibrium data fitted very well in the Langmuir isotherm equation, confirming the monolayer adsorption of MB with a monolayer adsorption capacity of 1,388 mg/g. This adsorption capacity of prepared AC for the adsorption of MB was higher that of AC cited in the literature. The pseudo-second-order kinetic model fitted well to describe the kinetic data of the adsorption process. The thermodynamic study depicted the exothermic and spontaneous nature of adsorption of MB onto prepared AC. The results suggested that the prepared AC could be applied as promising adsorbent to treat cationic dye containing wastewaters.

Declaration of competing interest

The authors declare no competing financial interest and manuscript is approved by all authors for publication.

Acknowledgement

The authors would like to thank SUST Research Centre for the grant (Project ID.: SUST/2016/AS 02) to conduct this work.

References

[1] Z. Carmen, S. Daniela, Textile Organic Dyes – Characteristics, Polluting Effects and Separation/Elimination Procedures from Industrial Effluents – A Critical Overview, T. Puzyn, A. Mostrag-Szlichtyng, Eds., Organic Pollutants Ten Years After the Stockholm Convention – Environmental and Analytical Update, InTechOpen, 2012, doi: 10.5772/32373.
[2] A. Regti, M.R. Laamari, S.-E. Stiriba, M. El Haddad, Use of response factorial design for process optimization of basic dye

adsorption onto activated carbon derived from Persea species, Microchem. J., 130 (2017) 129–136.
[3] M.T. Uddin, M.A. Islam, S. Mahmud, M. Rukanuzzaman, Adsorptive removal of methylene blue by tea waste, J. Hazard. Mater., 164 (2009) 53–60.
[4] S.S. Auerbach, D.W. Bristol, J.C. Peckham, G.S. Travlos, C.D. Hébert, R.S. Chhabra, Toxicity and carcinogenicity studies of methylene blue trihydrate in F344N rats and B6C3F1 mice, Food Chem. Toxicol., 48 (2010) 169–177.
[5] J. Mittal, Permissible synthetic food dyes in India, Resonance, 25 (2020) 567–577.
[6] L. Tan, M. He, L. Song, X. Fu, S. Shi, Aerobic decolorization, degradation and detoxification of azo dyes by a newly isolated salt-tolerant yeast Scheffersomyces spartinae TLHS-SF1, Bioresour. Technol., 203 (2016) 287–294.
[7] X.Q. Yang, X.X. Zhao, C.Y. Liu, Y. Zheng, S.J. Qian, Decolorization of azo, triphenylmethane and anthraquinone dyes by a newly isolated *Trametes* sp. SQ01 and its laccase, Process Biochem., 44 (2009) 1185–1189.
[8] A. Mariyam, J. Mittal, F. Sakina, R.T. Baker, A.K. Sharma, A. Mittal, Efficient batch and fixed-bed sequestration of a basic dye using a novel variant of ordered mesoporous carbon as adsorbent, Arabian J. Chem., 14 (2021) 103186, doi: 10.1016/j.arabjc.2021.103186.
[9] D. Bousalah, H. Zazoua, A. Boudjemaa, A. Benmounah, K. Bachari, Degradation of indigotine food dye by Fenton and photo-Fenton processes, Int. J. Environ. Anal. Chem., (2020) 1–14, doi: 10.1080/03067319.2020.1786546.
[10] A. Tariq, S. Islam, I.A. Shaikh, M.W. Mushtaq, S. Ishaq, Performance assessment of alum as coagulant for degradation of disperse dyes from aqueous medium, Int. J. Environ. Anal. Chem., (2020), doi: 10.1080/03067319.2020.1806254.
[11] V.B.K. Mullapudi, A. Salveru, A.J. Kora, An in-house UV-photolysis setup for the rapid degradation of both cationic and anionic dyes in dynamic mode through UV/H_2O_2-based advanced oxidation process, Int. J. Environ. Anal. Chem., (2020), doi: 10.1080/03067319.2020.1800002.
[12] M.K. Oden, Treatment of CNC industry wastewater by electrocoagulation technology: an application through response surface methodology, Int. J. Environ. Anal. Chem., 100 (2020) 1–19.
[13] M.Z. Bin Mukhlish, M.A. Islam, M.A. Rahman, S. Hossain, M.A. Islam, M.T. Uddin, Facile solid-state synthesis of heterojunction CeO_2/TiO_2 nanocomposite as an efficient photocatalyst for the degradation of organic pollutants, Desal. Water Treat., 230 (2021) 169–183.
[14] H. Daraei, A. Mittal, Investigation of adsorption performance of activated carbon prepared from waste tire for the removal of methylene blue dye from wastewater, Desal. Water Treat., 90 (2017) 294–298.
[15] S.G. Muntean, A. Todea, S. Bakardjieva, C. Bologa, Removal of non benzidine direct red dye from aqueous solution by using natural sorbents: beech and silver fir, Desal. Water Treat., 66 (2017) 235–250.
[16] F. Yasin, T. Javed, M.I. Jilani, S. Zafar, M.I. Din, Adsorption of toxic crystal violet dye using rice husk: equilibrium, kinetic, and thermodynamic study, Desal. Water Treat., 227 (2021) 338–349.
[17] M.T. Uddin, Y. Nicolas, C. Olivier, T. Toupance, L. Servant, M.M. Müller, H.J. Kleebe, J. Ziegler, W. Jaegermann, Nanostructured SnO_2-ZnO heterojunction photocatalysts showing enhanced photocatalytic activity for the degradation of organic dyes, Inorg. Chem., 51 (2012) 7764–7773.
[18] Y. Anjaneyulu, N. Sreedhara Chary, D. Samuel Suman Raj, Decolourization of industrial effluents – available methods and emerging technologies – a review, Rev. Environ. Sci. Biotechnol., 4 (2005) 245–273.
[19] J.W. Lee, S.P. Choi, R. Thiruvenkatachari, W.G. Shim, H. Moon, Evaluation of the performance of adsorption and coagulation processes for the maximum removal of reactive dyes, Dyes Pigm., 69 (2006) 196–203.
[20] A. Singh, D.B. Pal, A. Mohammad, A. Alhazmi, S. Haque, T. Yoon, N. Srivastava, V.K. Gupta, Biological remediation technologies for dyes and heavy metals in wastewater treatment: new insight, Bioresour. Technol., 343 (2022) 126154, doi: 10.1016/j.biortech.2021.126154.
[21] A. Mittal, J. Mittal, Hen Feather: A Remarkable Adsorbent for Dye Removal, S.K. Sharma, Ed., Green Chemistry for Dyes Removal from Wastewater: Research Trends and Applications, Co-published by John Wiley & Sons, Inc., Hoboken, New Jersey, and Scrivener Publishing LLC, Salem, Massachusetts, Published Simultaneously in Canada, 2015, pp. 409–457. Available at: https://doi.org/10.1002/9781118721001.ch11
[22] A. Patel, S. Soni, J. Mittal, A. Mittal, C. Arora, Sequestration of crystal violet from aqueous solution using ash of black turmeric rhizome, Desal. Water Treat., 220 (2021) 342–352.
[23] J. Mittal, R. Ahmad, A. Mariyam, V.K. Gupta, A. Mittal, Expeditious and enhanced sequestration of heavy metal ions from aqueous environment by papaya peel carbon: a green and low-cost adsorbent, Desal. Water Treat., 210 (2021) 365–376.
[24] B. Haddad, A. Mittal, J. Mittal, A. Paolone, D. Villemin, M. Debdab, G. Mimanne, A. Habibi, Z. Hamidi, M. Boumediene, E. habib Belarbi, Synthesis and characterization of eggshell (ES) and eggshell with membrane (ESM) modified by ionic liquids, Chem. Data Collect., 33 (2021) 100717, doi: 10.1016/j.cdc.2021.100717.
[25] C. Arora, P. Kumar, S. Soni, J. Mittal, A. Mittal, B. Singh, Efficient removal of malachite green dye from aqueous solution using curcuma caesia based activated carbon, Desal. Water Treat., 195 (2020) 341–352.
[26] J. Mittal, R. Ahmad, A. Mittal, Kahwa tea (*Camellia sinensis*) carbon — a novel and green low-cost adsorbent for the sequestration of titan yellow dye from its aqueous solutions, Desal. Water Treat., 227 (2021) 404–411.
[27] M.Z. Bin Mukhlish, S. Hossain, A. Rahman, T. Uddin, Kinetic and equilibrium studies of the activated carbon prepared from jackfruit leaves for the adsorption of methyl orange, Desal. Water Treat., 256 (2022) 253–264.
[28] A.T.S. Konan, R. Richard, C. Andriantsiferana, K.B. Yao, M.H. Manero, Low-cost activated carbon for adsorption and heterogeneous ozonation of phenolic wastewater, Desal. Water Treat., 163 (2019) 336–346.
[29] M.S. Vohra, Adsorption-based removal of gas-phase benzene using granular activated carbon (GAC) produced from date palm pits, Arabian J. Sci. Eng., 40 (2015) 3007–3017.
[30] Ş. Yüksel, R. Orhan, The removal of Cr(VI) from aqueous solution by activated carbon prepared from apricot, peach stone and almond shell mixture in a fixed-bed column, Arabian J. Sci. Eng., 44 (2019) 5345–5357.
[31] M. Hosseinzehi, M. Khatebasreh, A. Dalvand, Modeling of Reactive Black 5 azo dye adsorption from aqueous solution on activated carbon prepared from poplar sawdust using response surface methodology, Int. J. Environ. Anal. Chem., (2020), doi: 10.1080/03067319.2020.1819991.
[32] S.A. Patil, U.P. Suryawanshi, N.S. Harale, S.K. Patil, M.M. Vadiyar, M.N. Luwang, M.A. Anuse, J.H. Kim, S.S. Kolekar, Adsorption of toxic Pb(II) on activated carbon derived from agriculture waste (Mahogany fruit shell): isotherm, kinetic and thermodynamic study, Int. J. Environ. Anal. Chem., (2020), doi: 10.1080/03067319.2020.1849648.
[33] O.O. Namal, E. Kalipci, Adsorption kinetics of methylene blue removal from aqueous solutions using potassium hydroxide (KOH) modified apricot kernel shells, Int. J. Environ. Anal. Chem., 100 (2020) 1549–1565.
[34] I.A.W. Tan, A.L. Ahmad, B.H. Hameed, Adsorption of basic dye on high-surface-area activated carbon prepared from coconut husk: equilibrium, kinetic and thermodynamic studies, J. Hazard. Mater., 154 (2008) 337–346.
[35] R.G. Pereira, C.M. Veloso, N.M. Da Silva, L.F. De Sousa, R.C.F. Bonomo, A.O. De Souza, M.O. Da Guarda Souza, R. Da Costa Ilhéu Fontan, Preparation of activated carbons from cocoa shells and siriguela seeds using H_3PO_4 and $ZnCl_2$ as activating agents for BSA and α-lactalbumin adsorption, Fuel Process. Technol., 126 (2014) 476–486.
[36] E.W. Nsi, A.E. Akpakpan, E.J. Ukpong, U.D. Akpabio, Preparation and characterization of activated carbon from

Hura crepitans Linn seed shells, Int. J. Eng. Sci., 5 (2016) 38–41.
[37] J. Yang, K. Qiu, Preparation of activated carbons from walnut shells via vacuum chemical activation and their application for methylene blue removal, Chem. Eng. J., 165 (2010) 209–217.
[38] J. Ndi Nsami, J. Ketcha Mbadcam, The adsorption efficiency of chemically prepared activated carbon from cola nut shells by $ZnCl_2$ on methylene blue, J. Chem., (2013), doi: 10.1155/2013/469170.
[39] M.B. Wu, R.C. Li, X.J. He, H.B. Zhang, W. Bin Sui, M.H. Tan, Microwave-assisted preparation of peanut shell-based activated carbons and their use in electrochemical capacitors, Xinxing Tan Cailiao/New Carbon Mater., 30 (2015) 86–91.
[40] P.Z. Guo, Q.Q. Ji, L.L. Zhang, S.Y. Zhao, X.S. Zhao, Preparation and characterization of peanut shell-based microporous carbons as electrode materials for supercapacitors, Wuli Huaxue Xuebao/Acta Phys. Chim. Sin., 27 (2011) 2836–2840.
[41] L.C. Romero, A. Bonomo, E.E. Gonzo, Acid-activated carbons from peanut shells: synthesis, characterization and uptake of organic compounds from aqueous solutions, Adsorpt. Sci. Technol., 21 (2003) 617–626.
[42] S. Soni, P.K. Bajpai, D. Bharti, J. Mittal, C. Arora, Removal of crystal violet from aqueous solution using iron based metal organic framework, Desal. Water Treat., 205 (2020) 386–399.
[43] S. Li, S. Xu, S. Liu, C. Yang, Q. Lu, Fast pyrolysis of biomass in free-fall reactor for hydrogen-rich gas, Fuel Process. Technol., 85 (2004) 1201–1211.
[44] E.P. Barrett, L.G. Joyner, P.P. Halenda, The determination of pore volume and area distributions in porous substances. I. Computations from nitrogen isotherms, J. Am. Chem. Soc., 73 (1951) 373–380.
[45] W.D. Harkins, G. Jura, Surfaces of solids. XII. An absolute method for the determination of the area of a finely divided crystalline solid, J. Am. Chem. Soc., 66 (1944) 1362–1366.
[46] A. Boonpoke, S. Chiarakorn, N. Laosiripojana, S. Towprayoon, A. Chidthaisong, Synthesis of activated carbon and MCM-41 from bagasse and rice husk and their carbon dioxide adsorption capacity, J. Sustain. Environ., 2 (2013) 77–81.
[47] Suhas, P.J.M. Carrott, M.M.L. Ribeiro Carrott, Lignin - from natural adsorbent to activated carbon: a review, Bioresour. Technol., 98 (2007) 2301–2312.
[48] B. Cagnon, X. Py, A. Guillot, F. Stoeckli, G. Chambat, Contributions of hemicellulose, cellulose and lignin to the mass and the porous properties of chars and steam activated carbons from various lignocellulosic precursors, Bioresour. Technol., 100 (2009) 292–298.
[49] S.J. Hitchcock, B. McEnaney, S.J. Watling, Fibrous active carbons from coir, J. Chem. Technol. Biotechnol. Chem. Technol., 33 (1983) 157–163.
[50] S. Joshi, B.P. Pokharel, Preparation and characterization of activated carbon from lapsi (*Choerospondias axillaris*) seed stone by chemical activation with potassium hydroxide, J. Inst. Eng., 9 (2014) 79–88.
[51] Y. Chen, B. Huang, M. Huang, B. Cai, On the preparation and characterization of activated carbon from mangosteen shell, J. Taiwan Inst. Chem. Eng., 42 (2011) 837–842.
[52] C. Saka, BET, TG-DTG, FT-IR, SEM, iodine number analysis and preparation of activated carbon from acorn shell by chemical activation with $ZnCl_2$, J. Anal. Appl. Pyrolysis, 95 (2012) 21–24.
[53] Y. Sudaryanto, S.B. Hartono, W. Irawaty, H. Hindarso, S. Ismadji, High surface area activated carbon prepared from cassava peel by chemical activation, Bioresour. Technol., 97 (2006) 734–739.
[54] D. Angin, E. Altintig, T.E. Köse, Influence of process parameters on the surface and chemical properties of activated carbon obtained from biochar by chemical activation, Bioresour. Technol., 148 (2013) 542–549.
[55] K. Yang, J. Peng, H. Xia, L. Zhang, C. Srinivasakannan, S. Guo, Textural characteristics of activated carbon by single step CO_2 activation from coconut shells, J. Taiwan Inst. Chem. Eng., 41 (2010) 367–372.
[56] H. Mao, D. Zhou, Z. Hashisho, S. Wang, H. Chen, H. Wang, Preparation of pinewood- and wheat straw-based activated carbon via a microwave-assisted potassium hydroxide treatment and an analysis of the effects of the microwave activation conditions, BioResources, 10 (2015) 809–821.
[57] R.L. Tseng, S.K. Tseng, Pore structure and adsorption performance of the KOH-activated carbons prepared from corncob, J. Colloid Interface Sci., 287 (2005) 428–437.
[58] J. Andas, M.L.A. Rahman, M.S.M. Yahya, Preparation and characterization of activated carbon from palm kernel shell, IOP Conf. Ser.: Mater. Sci. Eng., 226 (2017), doi: 10.1088/1757-899X/226/1/012156.
[59] R.M. Shrestha, Effect of preparation parameters on methylene blue number of activated carbons prepared from a locally available material, J. Inst. Eng., 12 (2017) 169–174.
[60] L. Khezami, A. Chetouani, B. Taouk, R. Capart, Production and characterisation of activated carbon from wood components in powder: cellulose, lignin, xylan, Powder Technol., 157 (2005) 48–56.
[61] S. Cheng, L. Zhang, H. Xia, J. Peng, J. Shu, C. Li, Ultrasound and microwave-assisted preparation of Fe-activated carbon as an effective low-cost adsorbent for dyes wastewater treatment, RSC Adv., 6 (2016) 78936–78946.
[62] T. Otowa, Y. Nojima, T. Miyazaki, Development of KOH activated high surface area carbon and its application to drinking water purification, Carbon N.Y., 35 (1997) 1315–1319.
[63] S.S. Balaji, M. Sathish, Supercritical fluid processing of nitric acid treated nitrogen doped graphene with enhanced electrochemical supercapacitance, RSC Adv., 4 (2014) 52256–52262.
[64] Y. Ji, T. Li, L. Zhu, X. Wang, Q. Lin, Preparation of activated carbons by microwave heating KOH activation, Appl. Surf. Sci., 254 (2007) 506–512.
[65] Y. Gao, Q. Yue, B. Gao, Y. Sun, W. Wang, Q. Li, Y. Wang, Comparisons of porous, surface chemistry and adsorption properties of carbon derived from *Enteromorpha prolifera* activated by $H_4P_2O_7$ and KOH, Chem. Eng. J., 232 (2013) 582–590.
[66] A.H. Mahvi, A. Dalvand, Kinetic and equilibrium studies on the adsorption of Direct red 23 dye from aqueous solution using montmorillonite nanoclay, Water Qual. Res. J. Can., 55 (2020) 132–144.
[67] M.T. Uddin, M.A. Rahman, M. Rukanuzzaman, M.A. Islam, A potential low cost adsorbent for the removal of cationic dyes from aqueous solutions, Appl. Water Sci., 7 (2017) 2831–2842.
[68] M. Tamez Uddin, M. Rukanuzzaman, M. Maksudur Rahman Khan, M. Akhtarul Islam, Adsorption of methylene blue from aqueous solution by jackfruit (*Artocarpus heteropyllus*) leaf powder: a fixed-bed column study, J. Environ. Manage., 90 (2009) 3443–3450.
[69] U.J. Etim, S.A. Umoren, U.M. Eduok, Coconut coir dust as a low cost adsorbent for the removal of cationic dye from aqueous solution, J. Saudi Chem. Soc., 20 (2016) S67–S76.
[70] T.K. Sen, S. Afroze, H.M. Ang, Equilibrium, kinetics and mechanism of removal of methylene blue from aqueous solution by adsorption onto pine cone biomass of *Pinus radiata*, Water Air Soil Pollut., 218 (2011) 499–515.
[71] N. Gopal, M. Asaithambi, P. Sivakumar, V. Sivakumar, Adsorption studies of a direct dye using polyaniline coated activated carbon prepared from *Prosopis juliflora*, J. Water Process Eng., 2 (2014) 87–95.
[72] R. Aravindhan, J.R. Rao, B.U. Nair, Removal of basic yellow dye from aqueous solution by sorption on green alga *Caulerpa scalpelliformis*, J. Hazard. Mater., 142 (2007) 68–76.
[73] A. Hebeish, M.A. Ramadan, E. Abdel-Halim, A. Abo-Okeil, An effective adsorbent based on sawdust for removal of direct dye from aqueous solutions, Clean Technol. Environ. Policy, 13 (2011) 713–718.
[74] G. McKay, M.J. Bino, A.R. Altamemi, The adsorption of various pollutants from aqueous solutions on to activated carbon, Water Res., 19 (1985) 491–495.
[75] N. Ayawei, A.N. Ebelegi, D. Wankasi, Modelling and interpretation of adsorption isotherms, J. Chem., 2017 (2017), doi: 10.1155/2017/3039817.

[76] S.J. Allen, G. Mckay, J.F. Porter, Adsorption isotherm models for basic dye adsorption by peat in single and binary component systems, J. Colloid Interface Sci., 280 (2004) 322–333.
[77] I. Langmuir, The adsorption of gases on plane surfaces of glass, mica and platinum, J. Am. Chem. Soc., 40 (1918) 1361–1403.
[78] H.M.F. Freundlich, Over the adsorption in solution, J. Phys. Chem., 57 (1906) 385–471.
[79] M.A. Islam, M.J. Ahmed, W.A. Khanday, M. Asif, B.H. Hameed, Mesoporous activated carbon prepared from NaOH activation of rattan (*Lacosperma secundiflorum*) hydrochar for methylene blue removal, Ecotoxicol. Environ. Saf., 138 (2017) 279–285.
[80] Ü. Geçgel, O. Üner, G. Gökara, Y. Bayrak, Adsorption of cationic dyes on activated carbon obtained from waste *Elaeagnus stone*, Adsorpt. Sci. Technol., 34 (2016) 512–525.
[81] L. Borah, M. Goswami, P. Phukan, Adsorption of methylene blue and eosin yellow using porous carbon prepared from tea waste: adsorption equilibrium, kinetics and thermodynamics study, J. Environ. Chem. Eng., 3 (2015) 1018–1028.
[82] G. Karaçetin, S. Sivrikaya, M. Imamotlu, Adsorption of methylene blue from aqueous solutions by activated carbon prepared from hazelnut husk using zinc chloride, J. Anal. Appl. Pyrolysis, 110 (2014) 270–276.
[83] J.J. Gao, Y.B. Qin, T. Zhou, D.D. Cao, P. Xu, D. Hochstetter, Y.F. Wang, Adsorption of methylene blue onto activated carbon produced from tea (*Camellia sinensis* L.) seed shells: kinetics, equilibrium, and thermodynamics studies, J. Zhejiang Univ. Sci. B, 14 (2013) 650–658.
[84] V. Bello-Huitle, P. Atenco-Fernández, R. Reyes-Mazzoco, Adsorption studies of methylene blue and phenol onto pecan and castile nutshells prepared by chemical activation, Rev. Mex. Ing. Quim., 9 (2010) 313–322.
[85] H. Deng, L. Yang, G. Tao, J. Dai, Preparation and characterization of activated carbon from cotton stalk by microwave assisted chemical activation-application in methylene blue adsorption from aqueous solution, J. Hazard. Mater., 166 (2009) 1514–1521.
[86] O.S. Bello, I.A. Adeogun, J.C. Ajaelu, E.O. Fehintola, Adsorption of methylene blue onto activated carbon derived from periwinkle shells: kinetics and equilibrium studies, Chem. Ecol., 24 (2008) 285–295.
[87] B.H. Hameed, A.L. Ahmad, K.N.A. Latiff, Adsorption of basic dye (methylene blue) onto activated carbon prepared from rattan sawdust, Dyes Pigm., 75 (2007) 143–149.
[88] A.L. Ahmad, M.M. Loh, J.A. Aziz, Preparation and characterization of activated carbon from oil palm wood and its evaluation on methylene blue adsorption, Dyes Pigm., 75 (2007) 263–272.
[89] S. Soni, P.K. Bajpai, J. Mittal, C. Arora, Utilisation of cobalt doped iron based MOF for enhanced removal and recovery of methylene blue dye from waste water, J. Mol. Liq., 314 (2020), doi: 10.1016/j.molliq.2020.113642.
[90] C. Arora, S. Soni, S. Sahu, J. Mittal, P. Kumar, P.K. Bajpai, Iron based metal organic framework for efficient removal of methylene blue dye from industrial waste, J. Mol. Liq., 284 (2019) 343–352.
[91] S. Lagergren, About the theory of so-called adsorption of soluble substances (Zur theorie der sogenannten adsorption geloster stoffe), Kungliga Svenska Vetenskapsakademiens, Handlingar, 24 (1898) 1–39.
[92] Y.S. Ho, G. McKay, Pseudo-second-order model for sorption processes, Process Biochem., 34 (1999) 451–465.
[93] E. Errais, J. Duplay, F. Darragi, I. M'Rabet, A. Aubert, F. Huber, G. Morvan, Efficient anionic dye adsorption on natural untreated clay: kinetic study and thermodynamic parameters, Desalination, 275 (2011) 74–81.
[94] F. Krika, O. el F. Benlahbib, Removal of methyl orange from aqueous solution via adsorption on cork as a natural and low-coast adsorbent: equilibrium, kinetic and thermodynamic study of removal process, Desal. Water Treat., 53 (2015) 3711–3723.

Supporting information

The N_2 adsorption/desorption isotherms demonstrated in Fig. S2 exhibited both type I and IV isotherms with H4 hysteresis loop. According to IUPAC classification, type I isotherm and IV isotherm with H4 hysteresis loop are characteristic of microporous structure and micro-mesoporous material, respectively [1]. Accordingly, if substantial adsorption is occurred at low relative pressure, the initial part of the isotherm is type I corresponding to a microporous structure. The adsorption isotherm shape of type IV with an H4 type of hysteresis loop at intermediate and high relative pressure also indicates the existence of mesopores and slit-shaped pores.

The pore-size distribution is a characteristic of the internal structures of microporous and mesoporous carbons. The *t*-plot was used to estimate the volume of micro pores and specific surface area. Fig. S2B demonstrated that the prepared activated carbon (AC) was micro-mesoporous in nature. The presence of meso-microporous structure in the prepared AC contributes to the enhanced adsorption of large molecules.

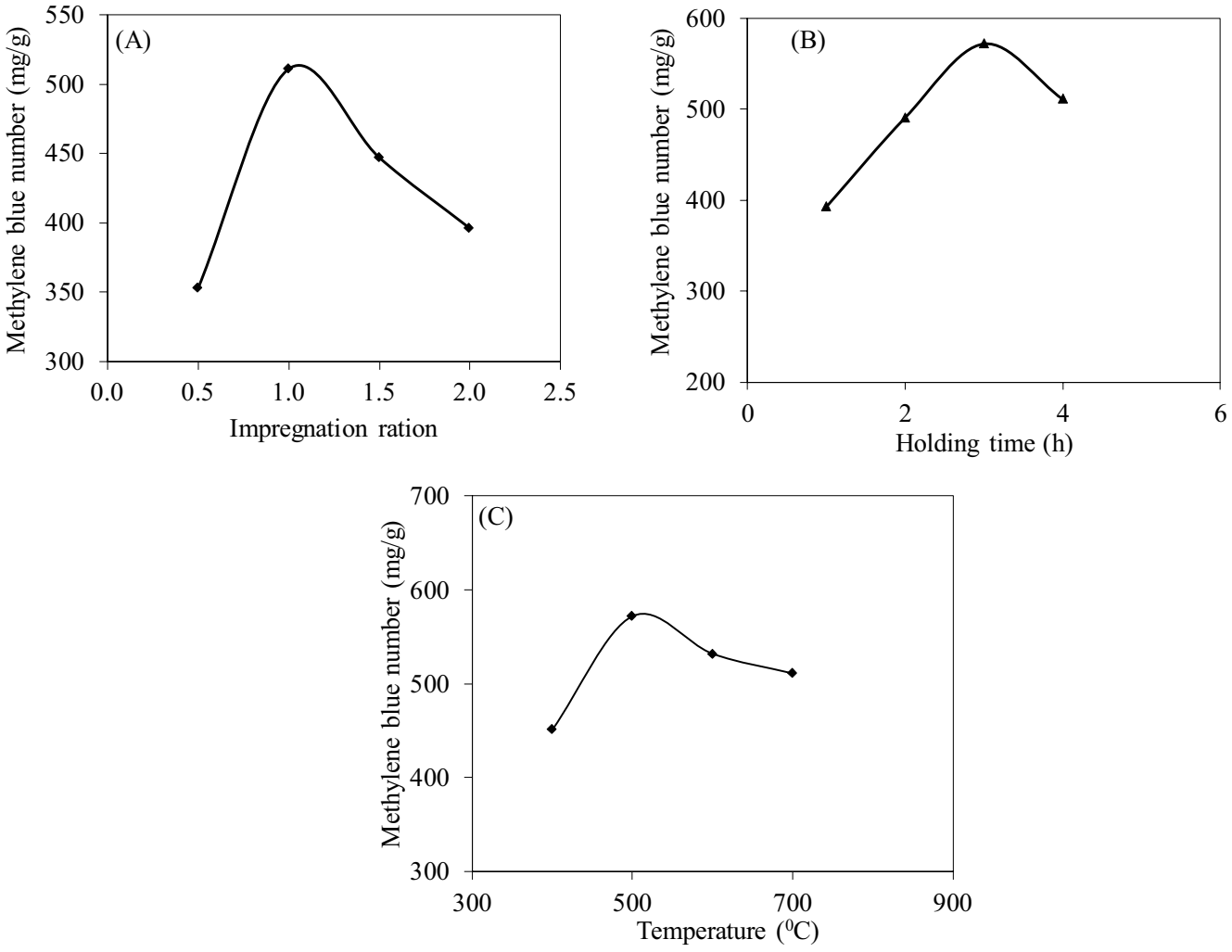

Fig. S1. Effect of (A) impregnation ratio, (B) holding time and (C) temperature on the methylene blue number of prepared activated carbon.

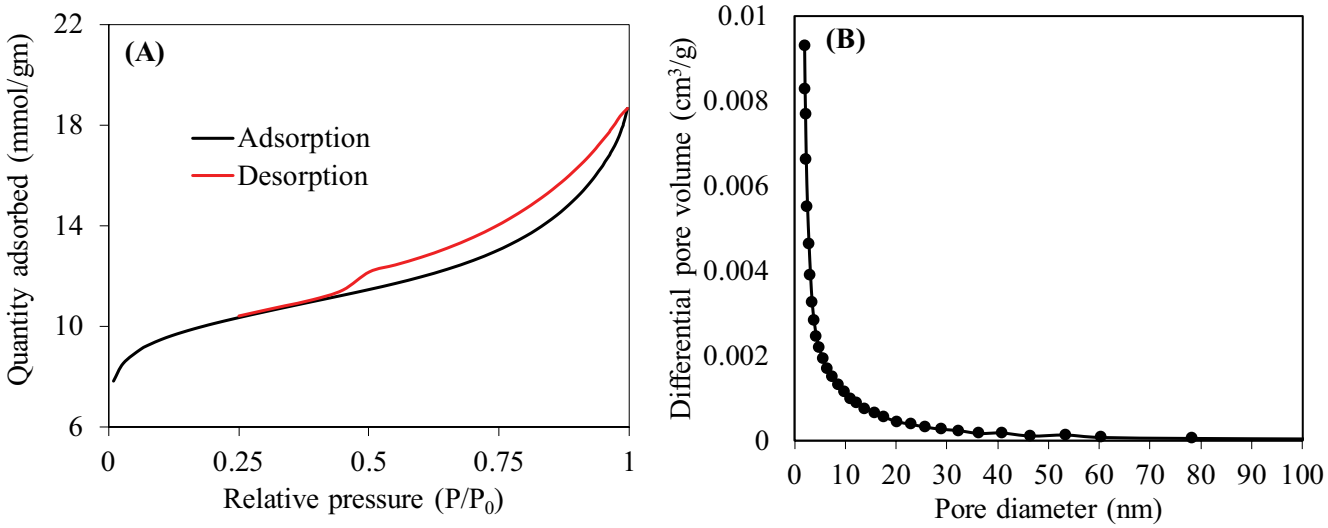

Fig. S2. (A) N_2 adsorption–desorption isotherm plots and (B) pore-size distribution of prepared activated carbon.

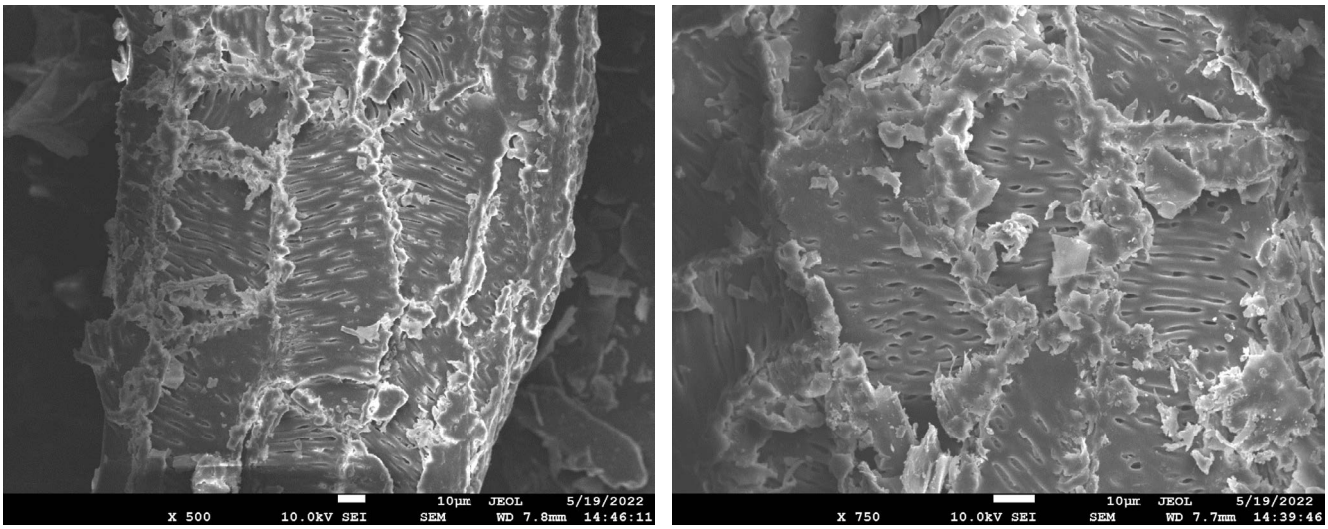

Fig. S3. SEM images of peanut shell powder before activation with KOH.

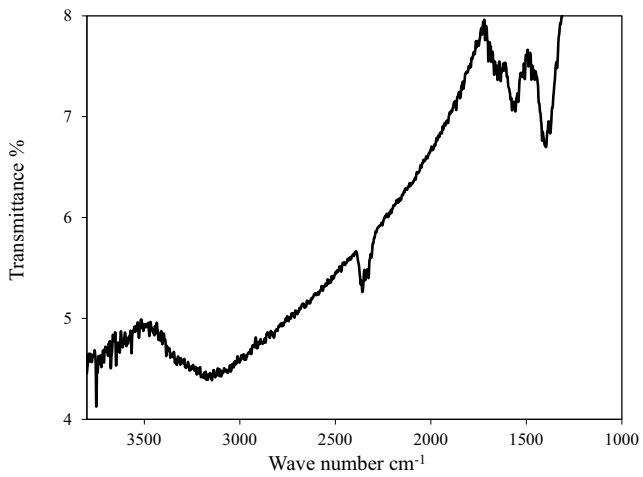

Fig. S4. FTIR spectra of activated carbon prepared from peanut shell.

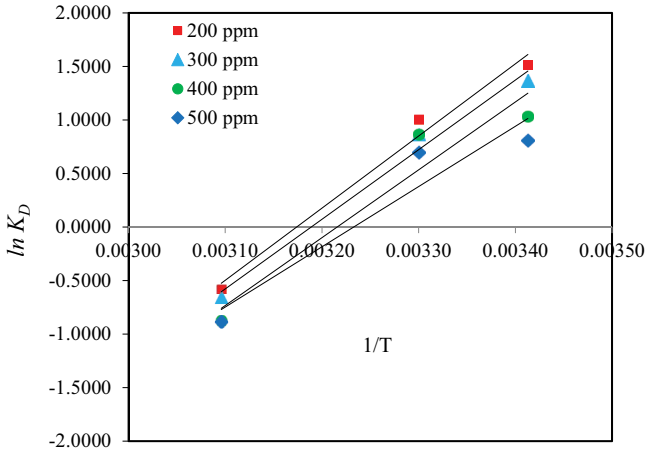

Fig. S5. Plot of $\ln K_D$ vs. $1/T$ for the estimation of the thermodynamic parameters for methylene blue adsorption using prepared activated carbon.